

Cascaded Förster Resonance Energy Transfer and Role of the Relay Dye

C. K. R. Namboodiri*, P. B. Bisht*, and V. R. Dantham†

Department of Physics, Indian Institute of Technology Madras, Chennai, 600036, India.

**E-mail: bisht@iitm.ac.in*

Tel. +91-44-2257-4866, Fax: +91-44-2257-4852

The effect of introducing a relay dye on the energy transfer efficiency in a new donor-acceptor system has been studied. The values of the critical transfer distance, the reduced concentration, and the energy transfer efficiency of the cascaded system (consisting of three dyes- donor-relay dye-acceptor) are compared with that of the two dye system. Experimentally, it has been observed that the presence of a relay dye increases the transfer efficiency from the donor to the acceptor.

Keywords: Cascaded Förster resonance energy transfer, Relay dye, Transfer efficiency.

** Current Address: Department of Science & Mathematics, Regional Institute of Education Mysore, Mysore, 570006, India.

† Current Address: Department of Physics, Indian Institute of Technology Patna, Patna, 800013, India.

1. Introduction

Förster resonance energy transfer (FRET) is a distance dependent, non-radiative energy transfer based on the dipole-dipole interaction [1, 2]. FRET is being widely used in the study of protein-protein interaction [3, 4], protein folding [5-7], photosynthetic systems [8, 9], bioimaging [10, 11], and developing FRET based sensors [12-14]. Cascaded (multi-step or multi-color) FRET is a recent advance in this field and has advantages compared with the traditional two-color FRET such as wide range of absorption of sunlight [15] and its efficient conversion of light to the deep red region in luminescent solar concentrators (LSCs) [16], decreased photodegradation of the donor dyes [8], efficient single molecule detection [17], and simultaneous detection of multiple metal ions [18]. Here, light from the donor gets transferred to the acceptor mainly through a relay dye (Panel (B), Figure 1). Cascaded FRET is helpful for the conversion of light at a shorter wavelength to a much longer wavelength which has applications in solar cells. For such an efficient light conversion, the choice of a relay dye is crucial as it affects the overall transfer efficiency. Hence, the role of the relay dye on the energy transfer efficiency needs to be investigated. In view of this, steady-state as well as time-resolved measurements of a standard dye-pair along with a relay dye has been carried out. In this study, Calcein and DTTCI were chosen as the donor (D) and acceptor (A_1) dyes, respectively. DODCI (R_1) was chosen as the relay dye because of its absorption and fluorescence spectra falling in between the other two. For a comparison of the obtained results with this D- R_1 - A_1 system, two more cascaded systems (Calcein- DODCI- HITCI and Calcein- Rhodamine B- HITCI) have been studied. This study gives experimental confirmation that the presence of a relay dye improves the energy transfer efficiency from the donor to the acceptor.

2. Experimental

Calcein (CALN), (BDH Ltd.), 3,3'-diethyloxadicarbocyanine iodide (DODCI), (Serva), 3,3'- diethylthiacarbocyanine iodide (DTTCI), (Serva), rhodamine B (RhB), (Serva), and 1, 1', 3, 3, 3', 3'-hexamethylindotricarbocyanine iodide (HITCI), (Sigma- Aldrich) were used as received. The molecular structure of the dyes used are reported. Spectrograde methanol (Thomas- Bakers) and distilled water (Modern Distilled Water, Chennai) were used as received. Polyvinyl alcohol (PVA, molecular weight \approx 125000) was obtained from S. D. Fine-Chem. Ltd.,

Mumbai. 20 g of PVA in 200 ml of distilled water was stirred for half an hour at 300 K. Dye was mixed with PVA to obtain the uniform, bubble-free solution. PVA-dye solution was dispersed onto a slide glass, and was allowed to dry for 48 hours at room temperature to obtain the polymer samples. The entire FRET study was done using so obtained solid state PVA films of thickness around 100 μm .

Steady-state absorption spectra were recorded using a dual-beam absorption spectrometer (Jasco model V- 570). Fluorescence spectra were recorded using a Raman spectrometer (Horiba Jobin Yvon, HR 800) with a grating of 600 groves/mm. The samples were excited with 488 nm, Ar^+ laser. An objective lens of 100X was used for excitation. The fluorescence was collected with a Peltier cooled CCD (DU420A-OE-324, Andor Technologies) in a back scattering geometry after passing through an edge filter. The time of exposure was kept as 1 second for all measurements.

The time-resolved studies were done under *ps* excitation using the time-correlated single photon counting (TCSPC) technique, described elsewhere [19]. Briefly, a *ps* diode laser (50 *ps*, 470 nm, 1MHz, PiL047, Advanced photonics Systems, Germany) excites the sample and the fluorescence is collected in the back-scattering geometry by using an epifluorescence microscope (E400, Nikon) and is detected with a PMT (Hamamatsu R928). The decay curves were recorded with the help of a TCSPC card and software (T900, Edinburgh Instruments). Commercial software (FAST, Edinburgh Instruments) was used for data analysis. The goodness of the fit was judged by the value of the reduced chi-squared (χ^2) and the distributions of residuals.

3. Theoretical Aspects

The rate of FRET is given by [20],

$$k_{D^*A} = \frac{1}{\tau_D} \left(\frac{R_{0A}}{r_{DA}} \right)^6 \quad (1)$$

where, τ_D is the fluorescence lifetime of the pure donor, and R_{0A} is known as the critical transfer distance, and r_{DA} is the real distance between the donor and acceptor molecules. Mostly, the fluorescence decay of an excited fluorophore follows single exponential decay given by,

$$I_D(t) = I_0 \exp\left(-\frac{t}{\tau_D}\right) \quad (2)$$

In a donor- acceptor system, the donor decay follows the Förster expression given by [20],

$$I_D(t) = I_0 \exp\left[\left(-\frac{t}{\tau_D}\right) - 2\gamma_{DA}\left(\frac{t}{\tau_D}\right)^{\frac{1}{2}}\right] \quad (3)$$

where γ_{DA} is the ratio of the acceptor concentration to the critical acceptor concentration ($\gamma_{DA} = \frac{C_A}{C_{0A}}$) known as the reduced concentration.

Critical acceptor concentration is related to the critical transfer distance by,

$$C_{0A} = \frac{3000}{2\pi^{3/2}NR_{0A}^3} \quad (4)$$

The efficiency of the energy transfer (η) is calculated by [20],

$$\eta = \sqrt{\pi}\gamma_{DA} \exp(\gamma_{DA}^2)(1 - \text{erf}(\gamma_{DA})) \quad (5)$$

where the $\text{erf}(\gamma_{DA})$ is the Gaussian error function.

The decay of the acceptor follows the equation [20, 21],

$$I_A(t) = B_2 \exp\left(-\frac{t}{\tau_2}\right) - B_1 \exp\left(-\frac{t}{\tau_1}\right) \quad (6)$$

where τ_1 and τ_2 are the two lifetime components and B_1 and B_2 are the corresponding amplitudes.

4. Results & Discussions

4.1 Selection of dye system

Table I (a) gives the donor-donor (D-D) migration spectroscopic parameters of the dyes, used in this study. The dyes were so chosen that the overlap

integral for D-D migration varies by three orders of magnitude, from $0.05 \times 10^{-13} \text{ M}^{-1}\text{cm}^3$ (for CALN) to $33.9 \times 10^{-13} \text{ M}^{-1}\text{cm}^3$ (for HITCI). The corresponding variation of the critical transfer distance (R_{0self}) was from $24 \pm 1 \text{ \AA}$ to $69 \pm 1 \text{ \AA}$. The normalized absorption and normalized fluorescence spectra of the dyes in the polymer matrix (PVA) are shown in panel A of figure 1. It can be seen that the absorption and fluorescence spectra of these dyes cover the range of wavelengths from visible to near IR.

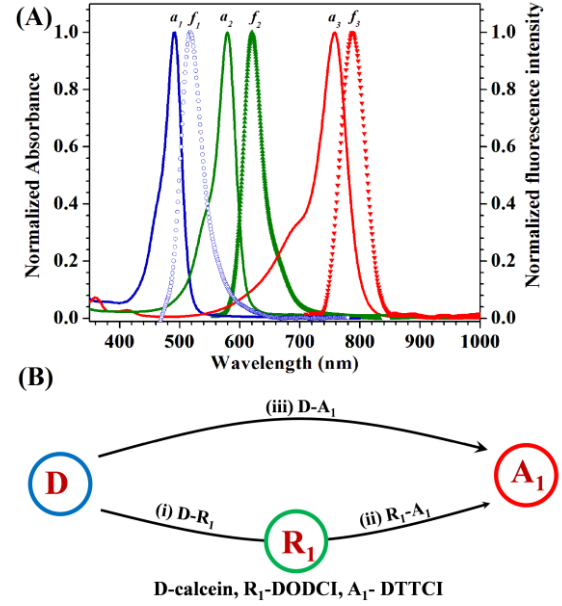


Figure 1. The normalized absorption (solid lines- $a_1, a_2,$ and a_3) and the fluorescence (symbols- $f_1, f_2,$ and f_3) spectra of CALN, DODCI, and HITCI respectively are shown in panel A. Panel B gives a schematic diagram of various FRET pathways in D-R₁-A₁ system.

Table I (b) gives the spectral overlap (J_{DA}) and R_{0A} values for various dye-pairs. Besides the large value of J_{DA} for CALN-RhB (D-R₂) and DODCI- DTTCI (R₁-A₁) systems, the values are small for other dye pairs because of wide separation between the fluorescence band of the donor and the absorption band of the acceptor.

4.2 Component dye pairs of the cascaded system

A cascaded system consists of 3 components, viz. D-R system, R-A system, and D-A system. Therefore, it is essential to study the properties of individual component systems

Table I (a). Various spectroscopic parameters of the dyes used.

	(a)	(b)	(c)	(d)
Dye	$\tau \pm 0.01$ (ns)	QY	$J_{self} \pm 0.01$ ($\times 10^{13} \text{ M}^{-1} \text{ cm}^3$)	$R_{0self} \pm 0.1$ (\AA)
D	3.43	0.38 ^(e)	0.05	24.4
R ₁	2.85	0.29 ^(f)	1.00	38.4
R ₂	3.65	0.69 ^(g)	0.30	34.1
A ₁	1.18 ^(h)	0.03 ⁽ⁱ⁾	30.00	47.3
A ₂	1.70 ^(j)	0.28 ^(k)	33.90	68.8

Table I (b). The spectral overlap and critical transfer distance for seven dye pairs

Dye pair	Spectral overlap $J_{DA} \pm 0.1$ ($\times 10^{13} \text{ M}^{-1} \text{ cm}^3$)	Critical transfer distance $R_{0A} \pm 0.1$ (\AA)
CALN-HITCI (D-A ₂)	0.4	34.8
CALN -DTTCI (D-A ₁)	0.5	35.8
RhB-HITCI (R ₂ -A ₂)	3.2	50.7
DODCI-HITCI (R ₁ -A ₂)	6.1	51.9
CALN -DODCI (D-R ₁)	22.6	67.5
DODCI-DTTCI (R ₁ -A ₁)	148.6	88.3
CALN -RhB (D-R ₂)	148.6	92.4

(a) lifetime, (b) quantum yield, (c) intramolecular spectral overlap, and (d) intramolecular critical transfer distance of the dyes. (e) is taken from ref. [22], (f) from ref. [23], (g) from ref. [24], (h) and (i) from ref. [25], (j) from ref. [26], and (k) from ref. [27].

4.2.1 Donor- relay dye (D-R₁) system

The spectral overlap of this dye pair (D-R₁) is shown by the shaded region in the top panel of figure 2. The overlap integral and the corresponding critical energy transfer distance (R_{0A}) are given in Table I (b). The molar extinction coefficient of D is high ($\sim 5.5 \times 10^4 \text{ M}^{-1} \text{ cm}^{-1}$) and the ratio of the extinction coefficients of D to R₁ is 17 at the wavelength of excitation (488 nm).

This clearly indicates the dominant absorption of the excitation light by the donor.

The concentration of D was kept constant as 0.1 mM, while that of R₁ was varied from 0.1 mM to 1 mM. It can be seen that on increasing the concentration of R₁, the fluorescence intensity of D decreases with a subsequent increase in the fluorescence intensity of R₁ (bottom panel, figure 2). Since there is no diffusion in the PVA matrix, this observation is an indication of the

diffusion-less, resonance energy transfer between D and R_1 .

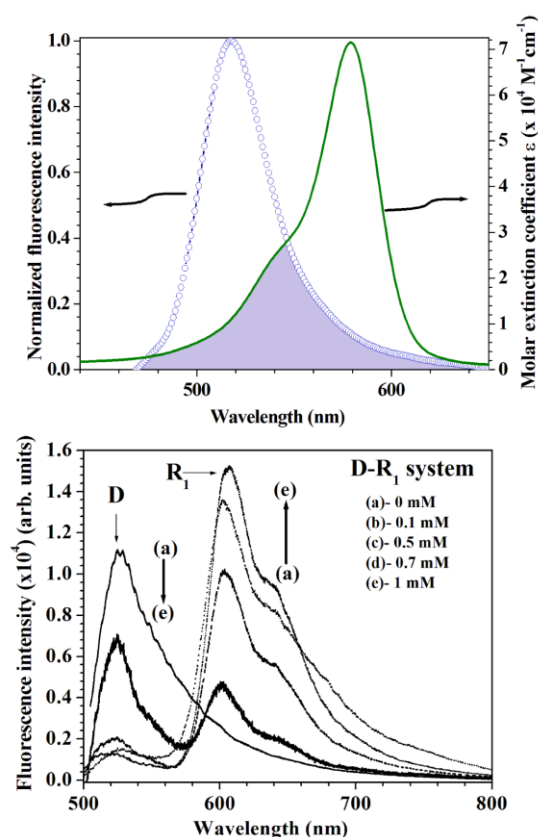


Figure 2. Fluorescence spectrum of donor (D) (\circ) and absorption spectrum of relay dye (R_1) (solid line) (top panel). The shaded region shows the spectral overlap. The fluorescence spectra of D- R_1 system are given in bottom panel for $[D] = 0.1$ mM. The relay dye concentrations are indicated in figure. The arrows indicate the peak positions for the fluorescence of D & R_1 .

Quenching of fluorescence can also take place because of several other reasons such as electron transfer [28], collisional quenching by oxygen, iodine, acrylamide and a number of metal ions [29]. Hence, by using steady-state measurements alone it is not possible to know the exact mechanism. In addition, whenever there is a spectral overlap between donor fluorescence and acceptor absorption, the phenomenon of radiative energy transfer can take place [30]. Therefore, the time-resolved measurements help clarify the underlying mechanism and were carried out for these systems.

The fluorescence decay of D at the wavelength of 520 nm exhibits single exponential behaviour with a time constant of 3.43 ± 0.01 ns. On increasing the concentration of R_1 the decay curves deviate from the

single exponential nature and fit with the Förster type function (equation (3)). The results of the analysis of the decay profiles are summarised in table II. It can be seen that the critical transfer distance (R_{0A}) for R_1 concentration of 1 mM, is smaller (47 \AA) than that calculated (67.5 \AA) from the steady-state spectral overlap. The maximum efficiency obtained for this system was $\sim 38 \%$, corresponding to an acceptor concentration of 1 mM.

4.2.2 Relay dye- acceptor (R_1 - A_1) system

There exists considerable overlap between the fluorescence spectrum of R_1 and the absorption spectrum of A_1 leading to the large value of the overlap integral (Table I(b)). Therefore, this dye-pair of DODCI (R_1) and DTTCl (A_1) was selected as the relay dye-acceptor system. The overlap region is shown by the shaded region in the top panel, figure 3.

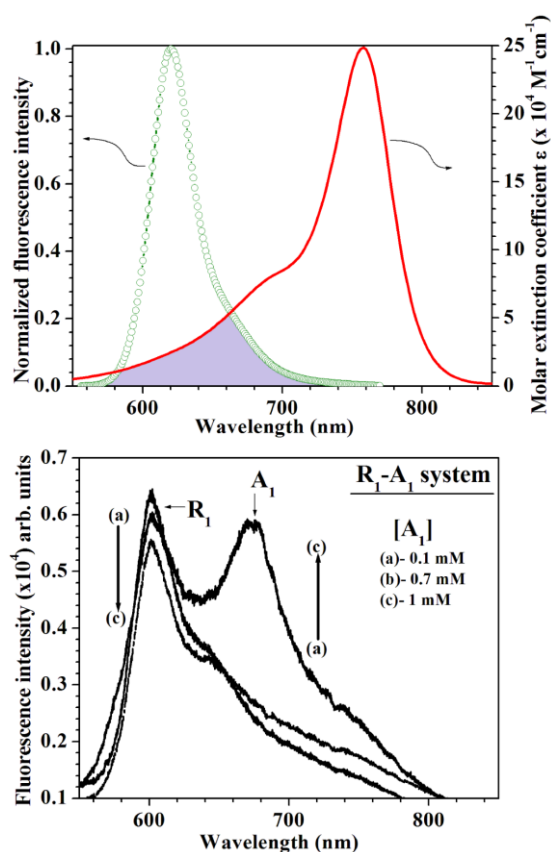


Figure 3. Fluorescence spectrum of relay dye (R_1) (\circ) and absorption spectrum of acceptor (A_1) (solid line) (top panel). The shaded region shows the spectral overlap. The fluorescence spectra of R_1 - A_1 system are given in bottom panel for $[R_1] = 0.1$ mM. The acceptor concentrations are indicated in figure. The arrows indicate the peak positions for the fluorescence of R_1 & A_1 .

Steady-state measurements have indicated the presence of FRET between R₁ and A₁ (bottom panel, figure 3). However, it was noticed that even in the presence of excitation energy transfer at higher acceptor concentration, the fluorescence intensity of the A₁ is not prominent. This is due to the low value of the quantum yield of NIR dyes. An increased probability of non-radiative decay as well as a decreased probability of radiative transitions at longer wavelength has been

reported for most of the NIR dyes [31, 32]. Also it can be seen that the D-D overlap integral for the longest wavelength acceptors are more than the other dyes. This large self-absorption effects play an important role in deciding the final efficiency of FRET in the cascaded system.

Table II. The decay profile analysis of the D-R₁, R₁-A₁, and D-A₁ systems ($\lambda_{exc}=470$ nm, $\lambda_{em}=520$ nm).

[Acceptor] (mM)	Single exponential fit		Förster fit			$R_{0A} \pm 0.1$ (Å)	η (%)
	τ_D (ns)	χ^2	τ_D (ns)	γ_{DA}	χ^2		
D-R₁ System							
0.5	3.10	1.10					
1	2.35	1.37	3.19	0.232	1.11	47	38.5
R₁-A₁ System							
0.1	1.81	1.15					
1	1.757	1.589	3.253	0.446	1.035	66	50.9
D-A₁ System							
1	3.83	1.12					
3	3.05	1.21	4.31	0.231	1.03	32.5	38.4

Table II gives the results of time-resolved measurements for R₁-A₁ system. The maximum efficiency is observed to be ~51% at $[A_1] = 1$ mM. However, there is some difference in the R_{0A} values obtained by time-resolved analysis is ~ 66 Å and spectroscopic measurements (~88 Å).

4.2.3 Donor- acceptor (D-A₁) system

The CALN (D) and DTTCl (A₁) dye system has low value of the overlap integral (overlap region is shown by the shaded region of the top panel of figure 4) and the critical transfer distance. This is due to the large shift between the donor fluorescence and acceptor

absorption (panel (A), figure 1). The fluorescence spectra of D with varying concentrations of A₁ indicate that the fluorescence yield of the latter is small even at its highest concentration (bottom panel, figure 4).

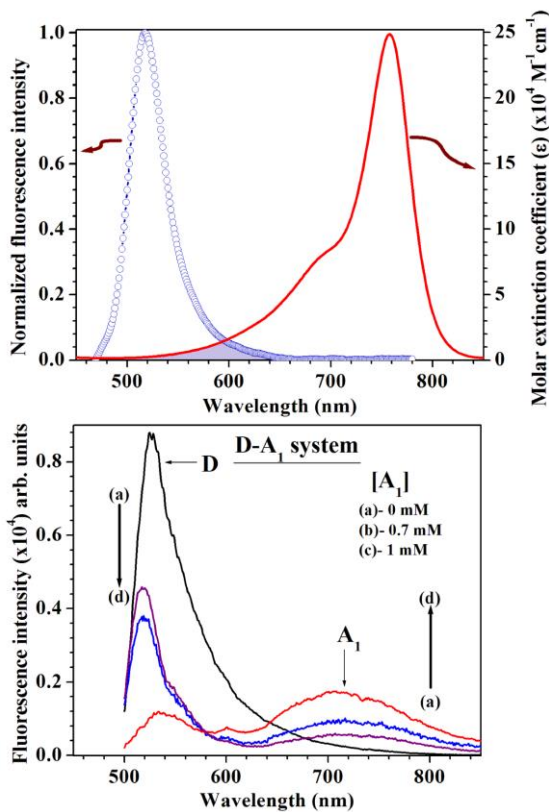


Figure 4. Fluorescence spectrum of donor (D) (\circ) and absorption spectrum of acceptor (A_1) (solid line) (top panel). The shaded region is the spectral overlap. The fluorescence spectra of D- A_1 system are given in bottom panel for $[D] = 0.1$ mM. The acceptor concentrations are indicated in figure. The arrows indicate the peak positions for the fluorescence of D & A_1 .

The fluorescence decay curves were recorded for this system at donor emission wavelength of 520 nm. The fluorescence decay of D exhibits single exponential behaviour with a time constant of 3.43 ± 0.01 ns (Table II). For lower concentrations of A_1 (up to ~ 3 mM), the decay curves follow the single-exponential behavior. A Förster function fit is obtained for higher concentrations. The R_{0A} value obtained from the time-resolved data (~ 32.5 Å) is slightly less than that obtained from spectroscopic measurements (~ 35.8 Å). For a concentration of $[A_1] = 3$ mM, the FRET efficiency is estimated to be 38.4%.

4.3. Cascaded system of three dyes

The fluorescence spectra for CALN-DODCI-DTTCI (D- R_1 - A_1) system by exciting at 488 nm is given in figure 5. For the cascaded system, the concentrations of D and R_1 were kept constant as 0.1 mM and 0.3 mM, respectively. It can be seen that, as the A_1 concentration is increased from 0 to 1 mM, the fluorescence intensity of D decreases with a concomitant increase in the intensity of A_1 . While fluorescence yield of A_1 was small for D- A_1 system, it is increased with the presence of the relay dye R_1 .

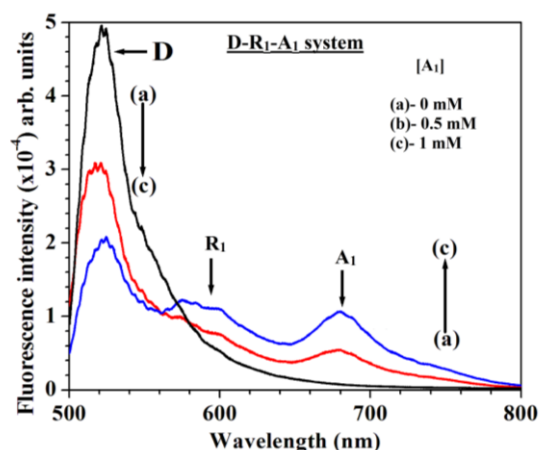


Figure 5. Fluorescence spectra of D- R_1 - A_1 system for $[D] = 0.1$ mM, and $[R_1] = 0.3$ mM and acceptor concentrations are as indicated in the figure. The arrows indicate the peak positions for the fluorescence of D, R_1 , & A_1 .

The fluorescence decay curves of this system were also recorded at the donor emission wavelength (520 nm). As shown in Table III, the decay profiles are single exponential for lower concentrations of A_1 . When the concentrations of R_1 and A_1 are increased, the decay profiles fit with Förster function (figure 6). The values of critical transfer distance (R_{0A}) and energy transfer efficiency (η) were calculated (equation (4) and (5)) from the value of reduced concentration (γ_{DA}) obtained by fitting the decay profiles. Corresponding to a typical acceptor concentration of 1 mM, the efficiency for this system was calculated to be $\sim 42\%$ (Table III) while there was no evidence of FRET in the case of D- A_1 system corresponding to the same acceptor concentration. Compared with the D- A_1 system with A_1 concentration of 3 mM, in the case of D- R_1 - A_1 system with A_1 concentration of even 1 mM, the obtained efficiency is more. This indicates that the presence of the relay dye R_1 enhances the energy transfer from D to A_1 .

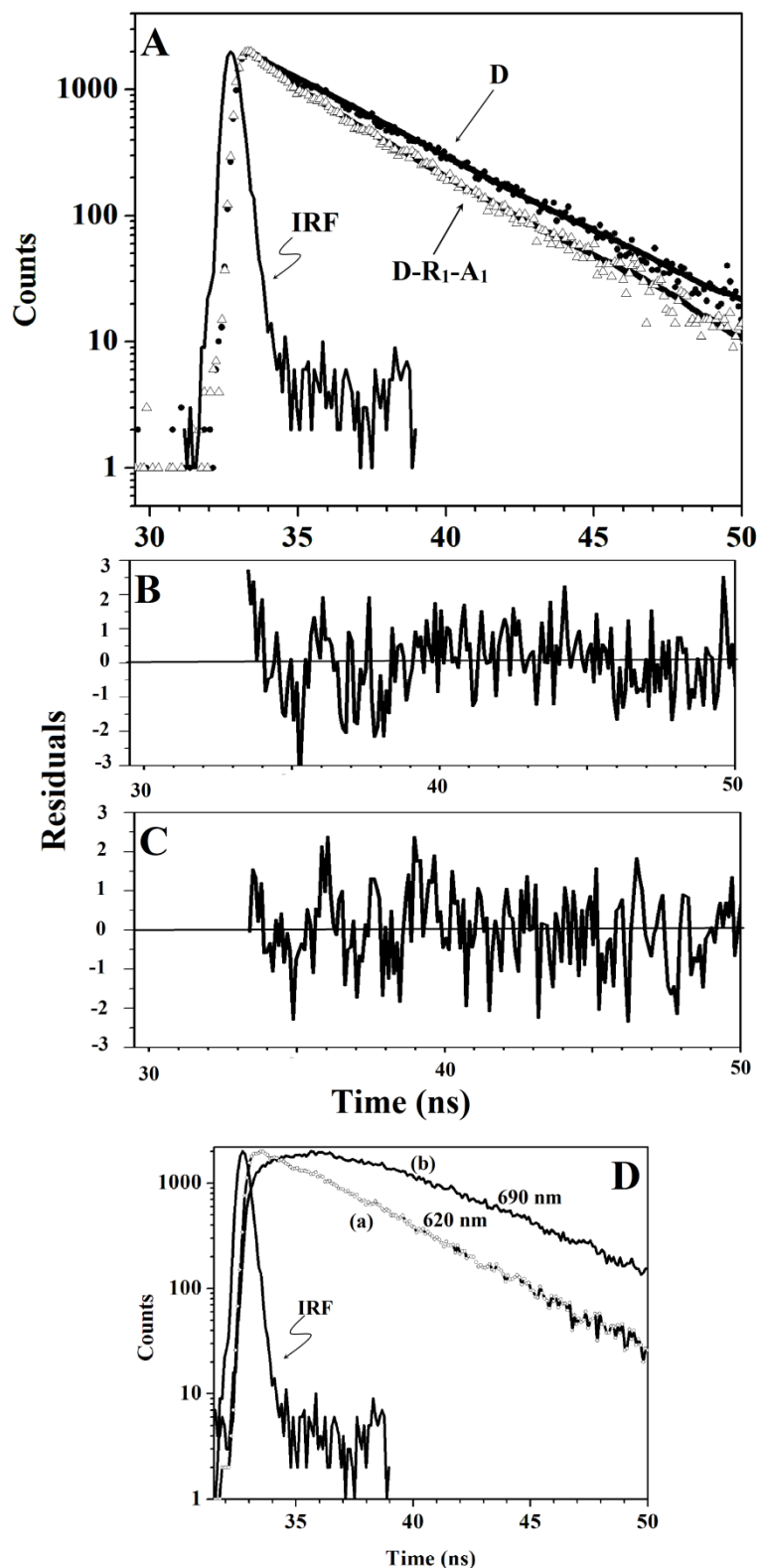


Figure 6. Panel A shows the fluorescence decay curves of D (0.1 mM) (●) and the D-R₁-A₁ system (Δ) at 520 nm with [R₁] = 1 mM and [A₁] = 5 mM. The solid lines show the single exponential fit for donor decay and Förster fit for the decay of the D-R₁-A₁ system, respectively. Panels B and C respectively show the residuals of the single exponential and Förster fits. Panel D shows fluorescence decay profiles of the D-R₁-A₁ system at the emission wavelength of 620 nm (a), and 690 nm (b) for the concentration same as in panel A.

Table III. The results of the time-resolved analysis with single exponential and Förster fit various dye systems. ($\lambda_{\text{exc}}= 470$ nm, $\lambda_{\text{em}}= 520$ nm)

System	Concentrations (mM)		Single exponential fit		Förster fit			$R_{0A} \pm 0.1$ (Å)	η (%)
			τ_D (ns)	χ^2	τ_D (ns)	γ_{DA}	χ^2		
D-R₁-A₁	[D] = 0.1	[A ₁] = 0	3.43	1.08					
	[R ₁] = 0.3	[A ₁] = 1.0	2.78	1.24	3.79	0.325	1.00	66.3	41.3
D-R₁-A₂	[D] = 0.1	[A ₂] = 0	3.43	1.08					
	[R ₁] = 0.3	[A ₂] = 2.0	1.15	3.41	1.68	2.511	1.03	96	92.9
D-R₂-A₂	[D] = 0.1	[A ₂] = 0	3.43	1.08					
	[R ₂] = 0.5	[A ₂] = 2.0	2.40	1.83	3.33	0.639	1.02	24.5	62.4

The decay profile of D-R₁ system, ($\lambda_{\text{em}}= 620$ nm) with [D] = 0.1 mM & [R₁] = 1 mM fits with $\tau_1= 0.93$ ns, $\tau_2= 2.97$ ns with coefficients -0.31 and 0.35, respectively ($\chi^2= 1.04$).

The decay profiles recorded at 620 nm and 690 nm were found to have the contributions of acceptor rise time as shown in panel D of figure 6.

4.4. Comparison with other cascaded FRET systems

In order to see the effect of various spectral parameters such as spectral overlap, and QY on the cascaded FRET efficiency, similar study was carried out with two other three-dye systems: CALN-DODCI-HITCI (D-R₁-A₂) and CALN-RhB-HITCI (D-R₂-A₂). The results of the time-resolved studies of these systems and associated component systems are summarised in table III. The overall transfer efficiency is maximum in the case of the second system (D-R₁-A₂). It was noticed that, compared with the first two systems, the third one (D-R₂-A₂) is better in terms of the fluorescence yield. This is because of the higher values of QY of R₂ and A₂ compared with that of R₁ and A₁, respectively. So, the selection of dyes with higher QY will benefit in getting more yield in applications where light needs to be converted from a shorter wavelength region to a longer wavelength region.

A high value of the spectral overlap in any one cascaded component system alone is not a sufficient condition to get a high value of overall transfer efficiency. The QY of the relay dye and the acceptor plays an important role in the final yield at longer wavelength. Another important factor is the orientation factor. It is to be noted that the orientation of the transition dipoles depend upon the molecular size, shape and symmetry. The value of κ^2 can vary between 0 and 4 even though it is taken as $\frac{2}{3}$ in the randomized donor and acceptor dipole cases [33].

5. Conclusions

The Förster resonance energy transfer between a dye pair with and without the presence of a relay dye has been studied. The study reveals that the presence of the relay dye (R₁) enhances the efficiency of energy transfer from the donor (D) to the acceptor (A₁). Experimentally it has been noticed that, a large value of the spectral overlap of one side - either donor to relay dye or relay dye to acceptor-alone is not sufficient for making the overall efficiency better. An additional parameter in increasing the final FRET yield can be an acceptor (A₁) with a higher QY. Therefore, this approach of cascaded energy transfer by selecting suitable dye-pairs with better efficiency can be used for efficient materials used in technological applications including solar devices.

Acknowledgement

We thank Department of Science and Technology (DST), New Delhi and Council of Scientific and Industrial Research (CSIR), New Delhi for financial support. Authors thank Dr. S. Mohan, for reading this manuscript.

References

- [1] T. Förster, *Discussions Faraday Soc.*, 27 (1959) 7-17.
- [2] U. Tripathy, P.B. Bisht, Effect of donor-acceptor interaction strength on excitation energy migration and diffusion at high donor concentrations, *The Journal of Chemical Physics*, 125 (2006) 144502-144508.
- [3] A.K. Kenworthy, Imaging Protein-Protein Interactions Using Fluorescence Resonance Energy Transfer Microscopy, *Methods*, 24 (2001) 289-296.
- [4] D. Llères, S. Swift, A.I. Lamond, Detecting Protein-Protein Interactions In Vivo with FRET using Multiphoton Fluorescence Lifetime Imaging Microscopy (FLIM), in: *Current Protocols in Cytometry*, John Wiley & Sons, Inc., 2001.
- [5] Y. Jia, D.S. Talaga, W.L. Lau, H.S.M. Lu, W.F. DeGrado, R.M. Hochstrasser, Folding dynamics of single GCN-4 peptides by fluorescence resonant energy transfer confocal microscopy, *Chemical Physics*, 247 (1999) 69-83.
- [6] B. Schuler, W.A. Eaton, Protein folding studied by single-molecule FRET, *Current Opinion in Structural Biology*, 18 (2008) 16-26.
- [7] S. Mahanta, R. Balia Singh, A. Bagchi, D. Nath, N. Guchhait, Study of protein-probe complexation equilibria and protein-surfactant interaction using charge transfer fluorescence probe methyl ester of N,N-dimethylamino naphthyl acrylic acid, *Journal of Luminescence*, 130 (2010) 917-926.
- [8] A.M. Mooney, K.E. Warner, P.J. Fontecchio, Y.-Z. Zhang, B.P. Wittmershaus, Photodegradation in multiple-dye luminescent solar concentrators, *Journal of Luminescence*, 143 (2013) 469-472.
- [9] J. Schäfer, R. Menzel, D. Weiß, B. Dietzek, R. Beckert, J. Popp, Classification of novel thiazole compounds for sensitizing Ru-polypyridine complexes for artificial light harvesting, *Journal of Luminescence*, 131 (2011) 1149-1153.
- [10] R.B. Sekar, A. Periasamy, Fluorescence resonance energy transfer (FRET) microscopy imaging of live cell protein localizations, *The Journal of Cell Biology*, 160 (2003) 629-633.
- [11] D. Ji, W. Lv, Z. Huang, A. Xia, M. Xu, W. Ma, H. Mi, T. Ogawa, Fluorescence resonance energy transfer imaging of CFP/YFP labeled NDH in cyanobacterium cell, *Journal of Luminescence*, 122-123 (2007) 463-466.
- [12] A.M. Dennis, G. Bao, Quantum dot-fluorescent protein pair as ratiometric pH sensor, in, 2010, pp. 75750C-75750C-75759.

- [13] N. Hildebrandt, K.D. Wegner, W.R. Algar, Luminescent terbium complexes: Superior Förster resonance energy transfer donors for flexible and sensitive multiplexed biosensing, *Coordination Chemistry Reviews*, 273–274 (2014) 125-138.
- [14] L. Feng, C. Tong, Y. He, B. Liu, C. Wang, J. Sha, C. Lü, A novel FRET-based fluorescent chemosensor of β -cyclodextrin derivative for TNT detection in aqueous solution, *Journal of Luminescence*, 146 (2014) 502-507.
- [15] S.T. Bailey, G.E. Lokey, M.S. Hanes, J.D.M. Shearer, J.B. McLafferty, G.T. Beaumont, T.T. Baseler, J.M. Layhue, D.R. Broussard, Y.-Z. Zhang, B.P. Wittmershaus, Optimized excitation energy transfer in a three-dye luminescent solar concentrator, *Solar Energy Materials and Solar Cells*, 91 (2007) 67-75.
- [16] C. Botta, P. Betti, M. Pasini, Organic nanostructured host-guest materials for luminescent solar concentrators, *Journal of Materials Chemistry A*, 1 (2013) 510-514.
- [17] S. Hohng, S. Lee, J. Lee, M.H. Jo, Maximizing information content of single-molecule FRET experiments: multi-color FRET and FRET combined with force or torque, *Chemical Society Reviews*, 43 (2014) 1007-1013.
- [18] J. Xia, M. Lin, X. Zuo, S. Su, L. Wang, W. Huang, C. Fan, Q. Huang, Metal Ion-Mediated Assembly of DNA Nanostructures for Cascade Fluorescence Resonance Energy Transfer-Based Fingerprint Analysis, *Analytical Chemistry*, 86 (2014) 7084-7087.
- [19] P. Sandeep, P.B. Bisht, Concentration sensing based on radiative rate enhancement from a single microcavity, *Chemical Physics Letters* 415 (2005) 15–19.
- [20] U. Tripathy, P.B. Bisht, K.K. Pandey, Study of excitation energy migration and transfer in 3,3'-dimethyloxycarbocyanine iodide (DMOCI) and o-(6-diethylamino-3-diethylimino-3H-xanthen-9-yl) benzoic acid (RB) in thin films of polyvinyl alcohol, *Chemical Physics*, 299 (2004) 105-112.
- [21] P.B. Bisht, H.B. Tripathi, D.D. Pant, Reinvestigation of the photophysics of the 2-naphtholamine hydrogen-bonded system. I, *Chemical Physics*, 147 (1990) 173-187.
- [22] C. Beghetto, C. Renken, O. Eriksson, G. Jori, P. Bernardi, F. Ricchelli, Implications of the generation of reactive oxygen species by photoactivated calcein for mitochondrial studies, *European Journal of Biochemistry*, 267 (2000) 5585-5592.
- [23] S. Ghosh, S. Mandal, C. Banerjee, V.G. Rao, N. Sarkar, Photophysics of 3,3'-Diethyloxadicarbocyanine Iodide (DODCI) in Ionic Liquid Micelle and Binary Mixtures of Ionic Liquids: Effect of Confinement and Viscosity on Photoisomerization Rate, *The Journal of Physical Chemistry B*, 116 (2012) 9482-9491.
- [24] W. Görtz, H.H. Perkampus, Bestimmung absoluter Fluoreszenzquantenausbeuten mittels der Photo-Akustik-Spektroskopie, *Z. Anal. Chem.*, 316 (1983) 180-185.
- [25] A. Godavartya, E.M. Sevick-Muraca, M.J. Eppstein, Three-dimensional fluorescence lifetime tomography, *Med. Phys.*, 32.4 (2005) 992-1000.
- [26] K.C. Jena, P.B. Bisht, Excitation energy transfer in a weakly coupled system: Studies with time-resolved fluorescence microscopy and laser induced transient grating techniques, *Chemical Physics*, 314 (2005) 179-188.
- [27] K. Rurack, M. Spieles, Fluorescence Quantum Yields of a Series of Red and Near-Infrared Dyes Emitting at 600–1000 nm, *Anal. Chem.*, 83 (2011) 1232–1242.
- [28] T. Kobayashi, Y. Takagi, H. Kandori, K. Kemnitz, K. Yoshihara, Femtosecond intermolecular electron transfer in diffusionless, weakly polar systems: Nile blue in aniline and N,N-dimethylaniline, *Chemical Physics Letters*, 180 (1991) 416-422.
- [29] J. Lyklema, *Fundamentals of Interface and Colloid Science: Liquid-Fluid Interfaces*, Elsevier Science, 2000.
- [30] B. Valeur, M.N. Berberan-Santos, *Molecular Fluorescence: Principles and Applications*, Wiley, 2013.
- [31] A. Zastrow, Physics and applications of fluorescent concentrators: a review, *Optical Materials Technology for Energy Efficiency and Solar Energy Conversion XIII*, *Proceedings of the SPIE*, 2255 (1994) 534-547.
- [32] A. Zastrow, K. Heidler, R.E. Sah, V. Wittwer, A. Goetzberger, On the conversion of solar radiation with fluorescent planar concentrators /FPCs, in: *3rd Photovoltaic Solar Energy Conference*, 1981, pp. 413-417.
- [33] B.W. van der Meer, D.M. van der Meer, S.S. Vogel, Optimizing the Orientation Factor Kappa-Squared for More Accurate FRET Measurements, in: *FRET – Förster Resonance Energy Transfer*, Wiley-VCH Verlag GmbH & Co. KGaA, 2013, pp. 63-104.